

Singlet-triplet transition in a single-electron transistor at zero magnetic field

A. Kogan, G. Granger, M. A. Kastner*, and D. Goldhaber-Gordon†

Department of Physics, Massachusetts Institute of Technology, Cambridge, Massachusetts 02139

Hadas Shtrikman

Braun Center for Submicron Research, Weizmann Institute of Science, Rehovot, Israel 76100

We report sharp peaks in the differential conductance of a single-electron transistor (SET) at low temperature, for gate voltages at which charge fluctuations are suppressed. For odd numbers of electrons we observe the expected Kondo peak at zero bias. For even numbers of electrons we generally observe Kondo-like features corresponding to excited states. For the latter, the excitation energy often decreases with gate voltage until a new zero-bias Kondo peak results. We ascribe this behavior to a singlet-triplet transition in zero magnetic field driven by the change of shape of the potential that confines the electrons in the SET.

PACS numbers: PACS 73.23.Hk, 72.15.Qm, 73.23.-b

The discovery of the Kondo effect in SETs has led to a great deal of experimental and theoretical interest.¹ In a SET charge fluctuations between the confined droplet of electrons, called an artificial atom, and the leads are suppressed by charge and energy quantization, resulting in small conductance except at voltages for which the number of electrons N on the droplet increases to $N+1$. However, when the artificial atom has odd N , and thus necessarily possesses non-zero spin, the differential conductance at zero drain-source bias is large for all gate voltages at zero temperature. This enhanced conductance results from the formation of a new many-body ground state at low temperature, in which the electrons in the artificial atom are coupled in a singlet state to those in the leads.

Much attention has also been paid to Kondo features seen when N is even. Such features were first reported by Schmid *et al.*² at zero magnetic field. Later Sasaki *et al.*³ and van der Wiel *et al.*⁴ showed that Kondo enhancement of the zero-bias differential conductance occurs for even N when a singlet-triplet transition is induced by a magnetic field applied normal to the plane of the two-dimensional motion of the electrons. In these experiments the Kondo features are only seen close to the magnetic field that induces the singlet-triplet transition. While it seems likely that the features seen by Schmid *et al.* for even N result from a triplet ground state at zero magnetic field, this has been difficult to demonstrate, because these authors do not observe the singlet state. Kyriakidis *et al.*⁵ have observed singlet-triplet transitions in a lateral quantum dot with $N=2$ at large bias with a perpendicular magnetic field near 1 T. They infer that the critical magnetic field can be tuned with a gate voltage by introducing nonparabolicity in the confining potential well.

Kondo features are also found in SETs made with carbon nanotubes. Liang *et al.*⁶ find that nanotubes with even N may have a singlet ground state with inelastic co-tunneling features at nonzero bias or a triplet ground state with a Kondo peak at zero bias. Nygård *et al.*⁷ have studied a singlet-triplet transition induced by a magnetic

field. The latter authors point out that the peaks superimposed on the inelastic co-tunneling edges for even N are a new signature of Kondo physics.

In this article we report the observation of excited state Kondo features for both even and odd N . At even N our data suggests that the triplet excitation energy changes as the shape of the confining potential is varied, often giving rise to a singlet-triplet ground state transition at zero magnetic field. With this interpretation, we use our differential conductance measurements to determine the exchange interaction. We find that the exchange is of the same order as the average energy level spacing. This may explain why SETs usually do not show even-odd effects in their conductance peaks.⁸

The SET we have studied is similar to those used by Goldhaber-Gordon *et al.*^{9,10} The SET is created by imposing an external potential on a two-dimensional electron gas (2DEG) at the interface of a GaAs/AlAs heterostructure. Our 2DEG has a mobility of 91,000 cm²/(Vs) and a density of 7.3×10^{11} cm⁻²; these quantities are measured shortly after fabrication. Our heterostructures are shallower than those in Refs.^{9,10}, 16 instead of 20 nm, and the δ doping level is higher, 1.5×10^{13} cm⁻² instead of 1.0×10^{13} cm⁻², yet the carrier density and mobility differ by less than 10%. We create the confining potential with electrodes shown in Fig. 1a. Applying a negative voltage to the three confining electrodes depletes the 2DEG underneath them and forms two tunnel barriers separating a droplet of electrons from the 2DEG regions on either side, which act as the source and drain leads. The confinement caused by the electrodes is supplemented by shallow etching of the cap layer before the gate electrodes are deposited. We estimate that our droplet is about 100 nm in diameter and contains about 50 electrons.

In all of our experiments the voltage on the gate V_g is varied while those on the other three electrodes are held fixed. We measure the differential conductance by applying a small alternating voltage, as well as dc voltage V_{ds} , between the drain and source leads and measuring

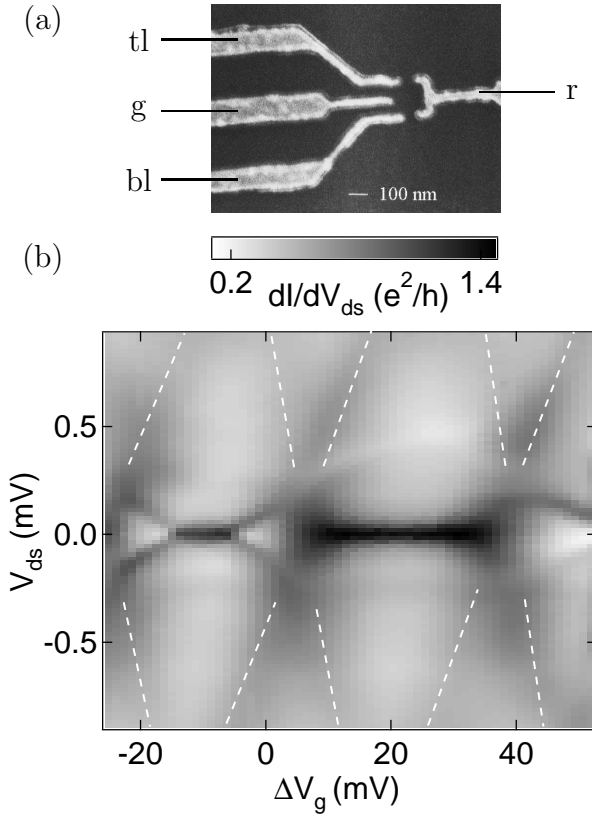


FIG. 1: (a) Electron micrograph of a device nominally identical to that used in this experiment. The voltages on the rightmost, top left, and bottom left electrodes are V_r , V_{tl} , and V_{bl} , respectively. That on the gate, V_g , is measured relative to a reference voltage V_0 . (b) Differential conductance dI/dV_{ds} in the V_{ds} - ΔV_g plane for $(V_r, V_{tl}, V_{bl}) = (-181.5, -155.9, -173.7)$ mV, and $V_0 = -172.7$ mV. The drain-source modulation was 48 μV_{p-p} . The dashed white lines are included as a guide to the eye to locate the Coulomb-blockade diamonds.

the current with a current preamplifier and a lock-in amplifier. While all the Kondo features near zero bias discussed in this paper can be clearly resolved with modulation of 10 μV peak-to-peak or less, we have used higher excitation voltages for some of the data to improve the signal-to-noise ratio at large dc biases between drain and source.

The effect of varying V_g is two fold. First, it tunes the electrochemical potential of the electrons in the droplet relative to Fermi energies in the leads. This allows us to vary N by changing the gate voltage.¹¹ Second, variations in V_g produce changes in the external potential confining the electrons, thus modifying the excitation spectrum. This much weaker effect is usually neglected, but it is central to the analysis of our results. In principle, these two effects can be separated experimentally by varying the voltage on several gates simultaneously.

Figure 1b shows the differential conductance of our SET for a range of $\Delta V_g = V_g - V_0$, over which two electrons are added to the artificial atom. The broad bands

forming a pair of diamonds result from the threshold for charge fluctuations induced by V_{ds} and ΔV_g . The sharp feature at $V_{ds} = 0$, present for $10 \text{ mV} \leq \Delta V_g \leq 40 \text{ mV}$, is identified as the Kondo peak for odd N. Thus, the unusual features in the adjacent diamonds are associated with even N.

In the left-hand diamond of Fig. 1b, we see, at the far left, two sharp peaks positioned symmetrically around $V_{ds} = 0$. As ΔV_g is increased the two peaks move together, until they merge to form a zero-bias peak. After remaining at zero bias for a range of ΔV_g , the two peaks separate again. Although we do not generally observe such symmetric patterns, we find similar behavior for most even N: sharp peaks separated by $\sim 100 \mu V$ from $V_{ds} = 0$ that shift with gate voltage at a rate such that the splitting disappears over $\sim 10 \text{ mV}$. When the splitting vanishes, a zero-bias Kondo peak results and remains at zero bias as ΔV_g is changed further.

We assume that when there is no zero-bias Kondo peak the ground state is the singlet and that for this situation the peaks observed symmetrically around $V_{ds} = 0$ result from Kondo screening of the excited-state triplet. We further assume that the shift of the peaks with gate voltage results from the change of energy separation of the lowest excited state from the ground state. That is, while all levels shift in energy at approximately the same rate because of the average electrostatic potential change caused by the gate, the transverse electric field, caused by the voltages between the plunger gate and the confining gates, affects each level of the artificial atom differently.

Note that, when eV_{ds} is equal to the energy difference between the ground state and first excited state of the artificial atom, one expects to see a threshold for inelastic co-tunneling, corresponding to a step in differential conductance. De Franceschi *et al.*¹² have recently reported such thresholds, although for their SETs the energies are only very weakly dependent on V_g . We observe peaks rather than thresholds, and the peaks are as sharp as those observed for zero-bias Kondo features, suggesting a strong Kondo screening of the excited triplet.

Hofstetter and Schoeller¹³ have calculated the evolution of the differential conductance for an artificial atom with single-channel leads and two orbitals, with energies ϵ_1 and ϵ_2 , as a function of the level spacing. Their Hamiltonian includes, for the excited state, a Heisenberg exchange interaction, $J\mathbf{S}_1 \cdot \mathbf{S}_2$, where \mathbf{S}_1 and \mathbf{S}_2 are the spins of the two electrons occupying the two orbitals. These authors predict that, when the level spacing is larger than $J/4$, two peaks should be seen in the differential conductance, displaced symmetrically from zero bias by the energy of the excited-state triplet relative to the singlet ground state, $\epsilon_t = |\epsilon_2 - \epsilon_1| - J/4$ when positive. However, when $\epsilon_t < 0$, the triplet becomes the ground state and a zero-bias Kondo peak is predicted.

Since our confining potential has low symmetry, we expect that all degeneracies are lifted. For simplicity we assume that the variation of ΔV_g results in a first-order shift in the orbital energies, as well as a coupling

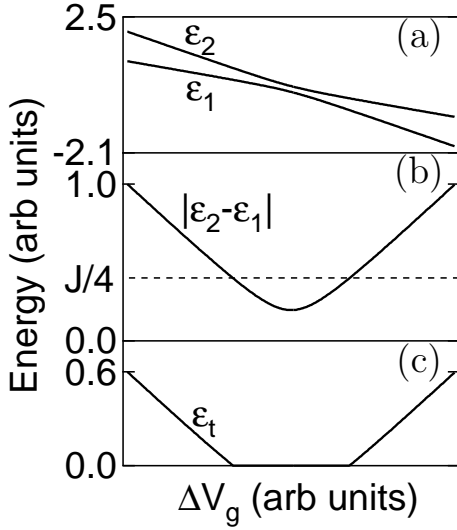


FIG. 2: Energy diagrams as discussed in the text for $\gamma_1 = 5$, $\gamma_2 = 10$, $\epsilon_1^0 = 1$, $\epsilon_2^0 = 2$, $\beta = 0.5$, and $J = 0.4$. (a) Two energy levels ϵ_1 and ϵ_2 as a function of ΔV_g . (b) Difference between the two levels. The dashed line gives the location of $J/4$. (c) Energy of the triplet relative to the ground state.

between the orbitals that is linear in ΔV_g . Ignoring all but the ground and first excited spatial states, we can estimate the evolution of the two levels with gate voltage by diagonalizing the two by two matrix \hat{H}_{st}

$$\hat{H}_{st} = \begin{pmatrix} \epsilon_1^0 - \gamma_1 \Delta V_g & \beta \Delta V_g \\ \beta \Delta V_g & \epsilon_2^0 - \gamma_2 \Delta V_g \end{pmatrix} \quad (1)$$

where ϵ_1^0 and ϵ_2^0 are the energies of the two spatial states at $\Delta V_g = 0$, $\gamma_1 \Delta V_g$ and $\gamma_2 \Delta V_g$ are the first-order shifts of the two states, and $\beta \Delta V_g$ is the coupling between them. The two resulting energies, ϵ_1 and ϵ_2 , are plotted as a function of ΔV_g in Fig. 2a. From these we find

$$|\epsilon_2 - \epsilon_1| = \sqrt{(\gamma_{12} \Delta V_g + [\epsilon_1^0 - \epsilon_2^0])^2 + 4\beta^2 \Delta V_g^2}, \quad (2)$$

where $\gamma_{12} \Delta V_g = \gamma_2 \Delta V_g - \gamma_1 \Delta V_g$. Subtracting $J/4$ gives ϵ_t ; we assume that J is independent of ΔV_g . $|\epsilon_2 - \epsilon_1|$ and ϵ_t are plotted in Fig. 2. For this choice of parameters, at both extremes of gate voltage, the singlet is the ground state, but near the anti-crossing the triplet is the ground state. This model thus explains features at $eV_{ds} = \epsilon_t$ like those in Fig. 1b.

Fitting the splitting between the two peaks at positive and negative V_{ds} in Fig. 1b to $2\epsilon_t$ we find $\gamma_{12} = (1.95 \pm 0.09) \times 10^{-2} e$, $|\epsilon_2^0 - \epsilon_1^0| = (0.25 \pm 0.08) \text{ meV}$, $\beta = (0.006 \pm 0.003) e$, and $J = (0.6 \pm 0.3) \text{ meV}$.

If β is large enough, ϵ_t is expected to remain positive for all ΔV_g and only the excited triplet Kondo features are expected. An example of this behavior is shown in Fig. 3. For this case we find $\gamma_{12} = (2.1 \pm 0.1) \times 10^{-2} e$, $|\epsilon_2^0 - \epsilon_1^0| = (0.4 \pm 0.2) \text{ meV}$, $\beta = (1.3 \pm 0.6) \times 10^{-2} e$, and J

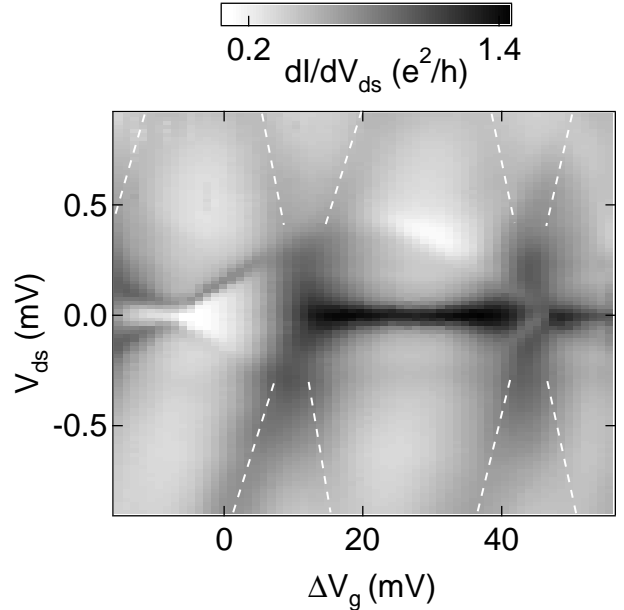


FIG. 3: Differential conductance dI/dV_{ds} in the V_{ds} - ΔV_g plane for voltages $(V_r, V_{tl}, V_{bl}) = (-191.4, -155.3, -155.3) \text{ mV}$ and $V_0 = -182.1 \text{ mV}$. The modulation on the drain-source voltage was $48 \mu\text{V}_{p-p}$. The dashed white lines are a guide to the eye for the Coulomb-blockade diamond edges.

$= (1.0 \pm 0.8) \text{ meV}$. Therefore, the two examples of Fig. 1b and Fig. 3 are well fitted with values of γ_{12} , β , and J that are the same within the errors. We note, however, that for nineteen other examples γ_{12} spans the range $0.5 \times 10^{-2} e$ to $2 \times 10^{-2} e$. It is likely that the difference in behavior between the case in Fig. 1b and that in Fig. 3 results from the distribution of level spacings.

We next discuss the parameters we have extracted. In a uniform external electric field, the quantity γ_{12} would be given by

$$\gamma_{12} = \frac{\langle 2|x|2 \rangle - \langle 1|x|1 \rangle}{d} e \quad (3)$$

where x is the lateral coordinate operator and the field is $\sim \Delta V_g/d$; d is the diameter of the artificial atom. In natural atoms, the orbitals have definite parity so $\gamma_{12} = 0$, but in our artificial atoms the potential does not have definite parity. Of course, the field is not uniform, but even if it were, the observed values of γ_{12}/e of order 1% would not be unreasonable.

For electrons in a GaAs 2DEG, Oreg *et al.*¹⁴ have estimated the ratio $\lambda = J/\Delta$ as a function of electron density, where Δ is the single-particle level spacing in the artificial atom. Their prediction is $\lambda = 0.22$ for our 2DEG density. Assuming the droplet diameter is 100 nm, we calculate $\Delta \approx 920 \mu\text{eV}$, which leads to $J \approx 0.2 \text{ meV}$. This is of the same order of magnitude as our measurement, albeit somewhat smaller.

The level separations we find are surprisingly small. Goldhaber-Gordon *et al.*¹⁰ found level spacings $\sim 400 \mu\text{eV}$ whereas our values of $|\epsilon_2 - \epsilon_1|$ are always $\lesssim 200$

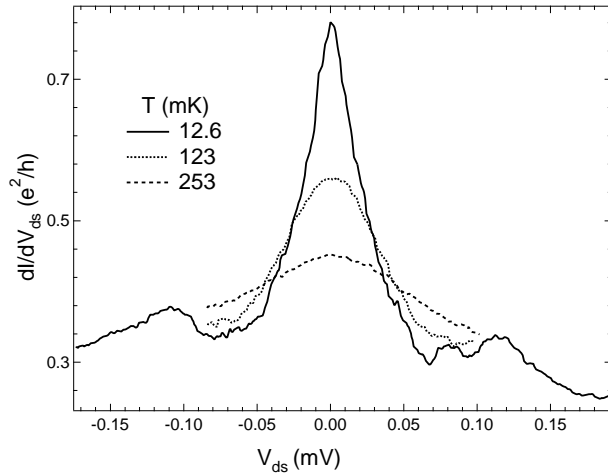


FIG. 4: Temperature dependence of dI/dV_{ds} as a function of V_{ds} for three different mixing chamber temperatures. The side bands are shown at the base temperature. The voltages on the electrodes are $(V_r, V_{tl}, V_{bl}, V_g) = (-181.5, -173.3, -173.3, -119.7)$ mV. The drain-source modulation was $10 \mu\text{V}_{p-p}$; we observe no significant change in the data down to $\sim 1 \mu\text{V}$ modulation.

μeV . This difference may result from the difference in size of the electron droplet, because of the different depth and doping of the two heterostructures. Our shallower, more heavily doped device would have a larger size leading to a smaller level spacing. This may explain why Goldhaber-Gordon *et al.* did not see triplet Kondo. However, even $400 \mu\text{eV}$ is a factor two smaller than expected from the estimated size of the droplet. Furthermore, one does not expect to observe charge quantization when the level spacing is smaller than the width of the levels at resonance, Γ , which we estimate from the width of the $V_{ds} = 0$ conductance peaks to be $\sim 500 \mu\text{eV}$. This small level spacing also leads to a disagreement with the theoretical prediction for J . If we use the spacing of $400 \mu\text{eV}$, we calculate $J \sim 0.1 \text{ meV}$ from Ref.¹⁴, much smaller than observed.

Occasionally, we observe excited state Kondo features for odd N , as well. Figure 4 shows one example. At the lowest temperature, one clearly sees side bands, sep-

arated from the central peak by about $100 \mu\text{eV}$, which are as sharp as the central Kondo peak. To our knowledge, data showing excited state Kondo features in a SET for odd N have not been published previously, although they were predicted long ago.¹⁵ From the temperature dependence of the central Kondo peak and the procedure of Goldhaber-Gordon *et al.*¹⁰, we find that the Kondo temperature for this particular gate voltage is 346 mK . The peak grows as temperature is lowered down to the base temperature. We have also measured the width of a Kondo peak as a function of temperature and find that it varies linearly with T down to 20 mK . Both these observations confirm that the electron temperature tracks the temperature of our refrigerator almost to the base value.

In conclusion, we are able to measure the energy of the triplet excited state and its dependence on gate voltage with high precision because the inelastic co-tunneling threshold and the concomitant Kondo peaks are much sharper than the Coulomb charging peaks. Very recently, M. Pustilnik and L. Glazman¹⁶ suggested an alternative explanation for our observations. They propose that the features we find at even N in this work could result from a nonconventional Kondo effect, predicted theoretically earlier¹⁷. This theory requires an $S=1$ ground state in a quantum dot coupled to two separate reservoirs, and predicts a non-monotonic temperature dependence of the zero-bias conductance. In particular, they find a suppressed conductance at zero temperature, in a sharp contrast with the predictions for the $S=1/2$ Anderson impurity model. To our knowledge, such behavior has not yet been observed experimentally. We are planning a detailed study of dI/dV_{ds} as a function of temperature to investigate whether the proposed mechanism indeed describes our devices.

We are grateful to W. Hofstetter, H. U. Baranger, M. Pustilnik, and L. I. Glazman for valuable discussions and to S. Amasha for experimental help. We also thank D. Mahalu for the electron-beam lithography. One of us (G.G.) acknowledges support from the National Sciences and Engineering Research Council of Canada. This work was supported by the US Army Research Office under Contract DAAD19-01-1-0637 and by the National Science Foundation under Grant No. DMR-0102153.

* mkastner@mit.edu

† Current address: Geballe Laboratory for Advanced Materials, McCullough Building, Room 346, 476 Lomita Mall, Stanford, California 94305-4045

¹ For a review see M. A. Kastner and D. Goldhaber-Gordon, Solid State Communications **119**, 245 (2001).

² J. Schmid, J. Weis, K. Eberl, and K. v. Klitzing, Physica B **256-258**, 182 1998; J. Schmid, J. Weis, K. Eberl, and K. v. Klitzing, Phys. Rev. Lett. **84**, 5824 (2000).

³ S. Sasaki, S. De Franceschi, J. M. Elzerman, W. G. van der Wiel, M. Eto, S. Tarucha, and L. P. Kouwenhoven, Nature

405, 764 (2000).

⁴ W. G. van der Wiel, S. De Franceschi, J. M. Elzerman, S. Tarucha, L. P. Kouwenhoven, J. Motohisa, F. Nakajima, and T. Fukui, Phys. Rev. Lett. **88**, 126803 (2002).

⁵ Jordan Kyriakidis, M. Pioro-Ladrière, M. Ciorga, A. S. Sachrajda, and P. Hawrylak, Phys. Rev. B **66**, 035320 (2002).

⁶ W. Liang, M. Bockrath, and H. Park, Phys. Rev. Lett. **88**, 126801 (2002).

⁷ J. Nygard, D. H. Cobden, and P. E. Lindelof, Nature **408**, 342 (2000).

⁸ D. S. Duncan, D. Goldhaber-Gordon, R. M. Westervelt,

- K. D. Maranowski and A. C. Gossard, Appl. Phys. Lett. **77**, 2183 (2000) and references therein.
- ⁹ D. Goldhaber-Gordon, H. Shtrikman, D. Mahalu, D. Abusch-Magder, U. Meirav, and M. A. Kastner, Nature **391**, 156 (1998).
- ¹⁰ D. Goldhaber-Gordon, J. Göres, M. A. Kastner, H. Shtrikman, D. Mahalu, and U. Meirav, Phys. Rev. Lett. **81**, 5225 (1998).
- ¹¹ L. P. Kouwenhoven, C. M. Marcus, P. L. McEuen, S. Tarucha, R. M. Westervelt, and N. S. Wingreen in *Mesoscopic Electron Transport*, NATO Advanced Study Institute, Series E, No 345, edited by L. L. Sohn, L. P. Kouwenhoven and G. Schoen (Kluwer, Dordrecht) 1997.
- ¹² S. De Franceschi, S. Sasaki, J. M. Elzerman, W. G. van der Wiel, S. Tarucha, and L. P. Kouwenhoven, Phys. Rev. Lett. **86**, 878 (2001).
- ¹³ W. Hofstetter and H. Schoeller, Phys. Rev. Lett. **88**, 016803 (2002).
- ¹⁴ Y. Oreg, P. W. Brouwer, X. Waintal, and B. I. Halperin, cond-mat/0109541 (unpublished).
- ¹⁵ T. Inoshita, Y. Kuramoto, and H. Sakaki, Superlattices and Microstructures **22**, 75 (1997).
- ¹⁶ M. Pustilnik and L. I. Glazman, private communication.
- ¹⁷ M. Pustilnik and L. I. Glazman, Phys. Rev. Lett. **87**, 216601 (2001).